METABOLIC PROFILING OF HUMAN TUMOR CELLS BY ISOTOPOMER ANALYSIS USING ^{13}C NMR SPECTROSCOPY.

Adriana Agnese Amaro

Department of Chemistry, Sapienza University of Rome

The present work is dedicated to the memory of Prof. Filippo Conti and Prof. Joseph P. Zbilut.   Prof. Conti introduced me to the study of NMR spectroscopy and metabolomics; Prof. Zbilut provided many people in Rome, including me, innumerable and precious suggestions for our scientific works.
Reminding both of them will always elicit in our mind a sense of gratitude for what they showed us in science and in everyday life.

ABSTRACT

This study concerns the analysis of human tumor cells metabolome HL60 and HL60-MX2 (Mitoxantrone resistant derivative of HL60 cell line displaying multidrug resistance) based on ^{13}C NMR spectroscopy. Our aim was: i) the possible evaluation of the mechanisms of action of antitumor drugs, and ii) the identification of the metabolic processes inducing sensibility or resistance to a specific drug in relation with the peculiar metabolic phenotype. We analysed the metabolic profiles of acute myeloid leukaemia (AML) cell lines, HL60 and HL60-MX2, by means of ^{13}C NMR mono and two-dimensional spectra, using [1,2-^{13}C$_2$]glucose as tracer for the isotopomer analysis. By comparing the analysis of key metabolites from the above lines it has been possible to describe and interpret the adaptation phenomena and the metabolic phenotypes of each cell line.

1. INTRODUCTION

Cancer, as a systemic disease, may be better understood through an integrated global profiling strategy.[12] This way, the "Achilles heel" of tumours is not a single gene-based event, but involves several regulatory pathways and the complex interplay of genetic, transcriptomic and metabolomic networks. It is well known that different cells and tissues with different basal metabolism, during tumorigenesis assume a common metabolic phenotype, generally defined as *Tumour Metabolome*, whose predominant feature is an alteration in glucose metabolism.

Simultaneous analysis of a large number of metabolites and enzymatic activities is an emerging and powerful approach to clarify pathological perturbations of metabolic pathways.[8]

As a matter of fact, the development of robust metabolomic platforms may greatly facilitate the understanding of the in vitro and in vivo actions of available

drugs and aid their incorporation into novel therapeutic settings.Profiling of metabolic activities is usually performed on cells fed with ^{13}C-labeled glucose, embedded in a large range of intermediary metabolites. As a result, each metabolite may exist as a collection of different isotopomers (differing in the ^{13}C molecular backbone position) reflecting the relative activities of pathways of production, as well as the functioning and metabolic phenotype of the analyzed system.[11,13]Thus, the tumour metabolome analysis becomes a key issue to understand global profiles of metabolic pathways under the influence of the developing and progressing cancer.[9, 21-22,30]

In this study we analyzed the metabolic profile of acute myeloid leukaemia cell lines HL60 and HL60-MX2. The latter one is a mitoxantrone resistant derivative clone of HL60 cell line. Metabolite levels have been used as metabolic biomarkers, while metabolic activities have been measured by metabolic fluxes: this provided direct evidence of changes in potential target pathways.

2. METHODS

2.1. *Isotopomers-based models*

In Metabolic Profiling analysis based on ^{13}C NMR spectroscopy, stable ^{13}C labeled isotopes are crucial. The use of stable isotopes allows obtaining measurement data to solve the flux analysis of a biological system, given a map of catabolic and anabolic networks.[31, 20, 17, 29, 7] Studying changes in the carbon labeling of compounds involved in metabolic pathways, allows to obtain information concerning the disease mechanism, physiology and phenotype. In contrast to the most common carbon isotope (^{12}C) which is not-NMR-detectable (it has no nuclear spin), the non-radioactive isotope ^{13}C does have a NMR-observable nuclear spin. However, since ^{13}C has extremely low natural abundance, feeding cells a metabolizable label containing ^{13}C is essential for detection and analysis. If cells are given a ^{13}C label (e.g [1,2-^{13}C$_2$]glucose)[1] the carbon label will enter the cell, and will be distributed among various compounds reflective the metabolic processes.[26] Thus, you may get a series of *isotopomers* for each intermediate, which means different isomers of the same molecule differing in number and position of isotopes ^{13}C.[6,10] It is important to underline that 13C NMR give the possibility to evaluate the position of ^{13}C carbons using the spin coupling information. (Fig. 1)

---

[1] Each isotopomer is indicated with m_1, m_2, m_n where 1,2, n is the number of ^{13}C atoms substituted in a molecule.
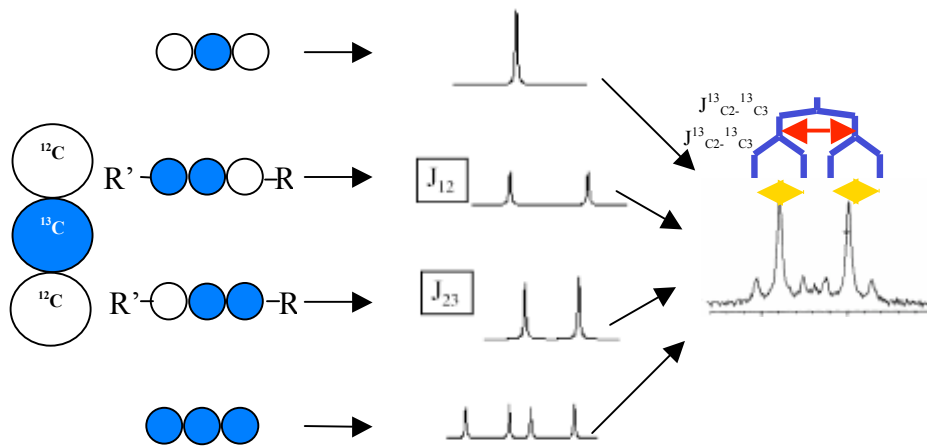
Figure 1. **Typical evolution of a ^{13}C NMR spectrum of a metabolite with 3 carbon atoms.** Blue circles represent labeled carbons, and white circles represent unlabeled carbons. Typically, if the adjacent carbons are unlabeled, only one ^{13}C will peak in the spectrum (singlet). If one of the two adjacent carbons is labelled, a doublet will be found, whose magnitude depends on the flanking functional groups. If both adjacent carbons are labelled, a double doublet will be seen on the spectrum. Considering only natural ^{12}C and its stable isotope ^{13}C, a molecule with a backbone of N carbons can exist as 2^N different isotopomers. For instance, in a molecule with 3 carbon atoms (e.g lactate), up to a maximum of 2^3 possible isotopomers are possible. Isotopomer analysis tells us whether a molecule is labeled in one, two (or more) positions, at the same time, and also where the labelled position(s) is/are. The molar fraction of each isotopomer represents the relative abundance with reference to any other possible isotopomer for the same molecule.[26, 31, 3, 17]

In order to dominate the cellular complexity we introduce a compartmental view of the system: metabolites are exchanged between different compartment pools. This is in marked contrast to single-cell microorganism analyses, where compartimentation is rarely included. Illustrative examples of this kind of work are the kinetic analysis of e.g. the glucose regulation by insulin, and lipoprotein metabolism.[1]

2.2. Quantification of isotopomers.

The interpretation of ^{13}C NMR spectra in terms of flux through metabolic pathway requires the quantification of the ^{13}C incorporated in specific carbons. This is normally done by expressing ^{13}C incorporation as an absolute ^{13}C enrichment in Ci carbon (YCi). The absolute ^{13}C enrichment YCi is defined as follows:

$$(YC_i)\,enrichment \ = \left[^{13}C\right]_m - \left[^{13}C\right]_{n.a.} \quad [1]$$

with:
$[^{13}C]_m = {}^{13}$C nM total quantity of a specific atom
$[^{13}C]_{n.a.} = {}^{13}$C nM in natural abundance of specific atom

The measurement of YCi involves the determination of ^{13}C concentration by the intensities of the signals for each metabolite in the spectrum and the

measurement of total concentrations. The ^{13}C enrichment in each carbon atom of different metabolites, can be measured by comparing the area of the peaks of interest with the area of an internal standard. The total amount of ^{13}C in a specific resonance signal is given by the formula

$$\left[^{13}C\right]_m = \left[^{13}C\right]_r \times \frac{(area)_m}{(area)_r} \qquad [2]$$

with:
$(area)_m$=integral value of each metabolite signal
$(area)_r$=integral value of reference signal
$[^{13}C]_m = {}^{13}C$ nM total quantity of a specific atom
$[^{13}C]_r = {}^{13}C$ nM in reference signal
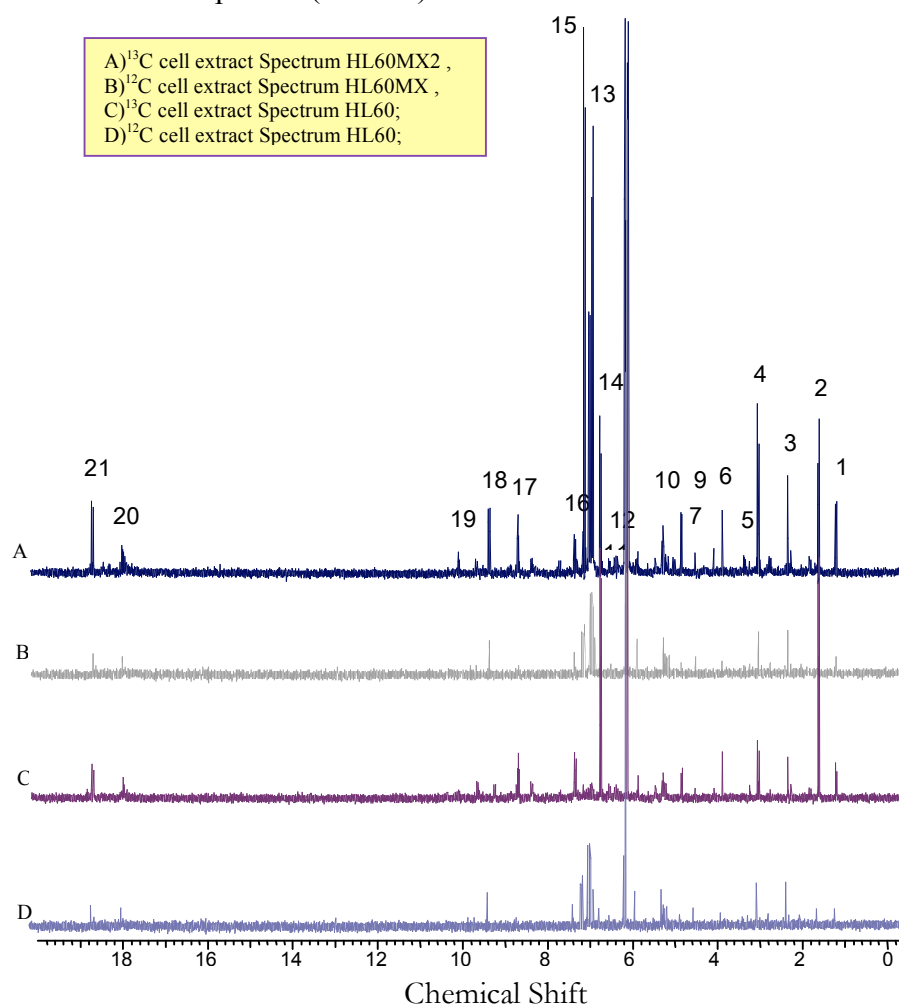
These expressions depend upon the following key assumptions:
(i) the various ^{13}C isotope isomers of the metabolic intermediates are in an isotopic steady state;
(ii) all reactions take place in compartments where metabolites are homogeneously distributed unless otherwise specified;
(iii) the stoichiometry of all biochemical reactions in the model is known;
(iv) complete biochemical knowledge on the fate of each carbon atom in the modelled reactions is available or can be inferred from the obtained ^{13}C-labeling data;
(v) ^{13}C isotope effects are absent, i.e., enzymes do not discriminate between ^{13}C-labeled and unlabeled metabolites.[31]

3. RESULTS

3.1. NMR Experiments

The metabolic profiles of HL60 and HL60-MX2 were determined using [1,2-$^{13}C_2$]glucose as tracer and the isotopomeric distribution through the study of ^{13}C NMR spectra of cellular extracts. (Figure 2)[11, 26, 20, 17, 5]

The metabolites identified in the ^{13}C NMR spectra, are shown in Table 1 .

The ^{13}C enrichments and intracellular isotopomeric distribution were determined from data in the ^{13}C spectra. (Table 2)

A) ^{13}C cell extract Spectrum HL60MX2 ,
B) ^{12}C cell extract Spectrum HL60MX ,
C) ^{13}C cell extract Spectrum HL60;
D) ^{12}C cell extract Spectrum HL60;

Figure 2. ^1H-decoupled ^{13}C-NMR spectra of HL60 & HL60MX2 cells.
3×10^8 cells per sample were incubated in the presence of ^{12}C- or [1,2-$^{13}C_2$]-glucose for 24 hours. The assignments of metabolites in ^{13}C spectra were made by comparing the carbon chemical shift with value in the literature. The concentration of metabolites was determined by integrating the peaks in ^{13}C spectra using ACDlab software, comparing with the integral of resonance peak of TSP that was treated as a standard, and normalizing to the total number of cells.

Peak #	Metabolite	^{13}C Position	Chemical Shift (ppm)
1	Alanine	C3	16.64
	Alanine	C2-C3	16.64
2	Lactate	C3	20.54
	Lactate	C2-C3	20.54
3	Glutamate	C3	27.41
	Glutamate	C2-C3	27.41
4	Glutamate	C4	33.93
	Glutamate	C3-C4-C5	33.93
	Glutamate	C4-C5	33.93
5	Aspartate	C3	37.00
	Aspartate	C2-C3	37.00
6	Glycine	C2	41.91
7	Malate	C3	43.81
8	Alanine	C2	50.99
	Alanine	C2-C3	50.99
9	Aspartate	C2	52.65
	Aspartate	C2-C3	52.65
10	Glutamate	C2	55.20
	Glutamate	C1-C2	55.20
	Glutamate	C2-C3	55.20
11	Serine	C3	56.81
	Serine	C2-C3	56.81
12	Serine	C2	60.64
	Serine	C2-C3	60.64
13	Lactate	C2	68.95
	Lactate	C2-C3	68.95
	Lactate	C1-C2-C3	68.95
14	αGlucose	C2	71.70
	αGlucose	C1-C2	71.70
15	βGlucose	C2	74.60
	βGlucose	C1-C2	74.60
16	Ribose-5-P	C4'-C5' (ATP)	84.28
17	Ribose-5-P	C1'(ATP)	87.28
	Ribose-5-P	C1'-C2'(ATP)	87.28
18	αGlucose	C1	92.55
	αGlucose	C1-C2	92.55
19	βGlucose	C1	96.34
	βGlucose	C1-C2	96.34
20	Glutamate	C1	175.01
	Glutamate	C1-C2	175.01
21	Glutamate	C5	181.84
	Glutamate	C4-C5	181.84

Table 1. Peak assignment from   cell extract ^{13}C NMR spectra in Figure 2

INTRACELLULAR ISOTOPOMERIC DISTRIBUTION					
Metabolites	^{13}C Position	Chemical Shift (ppm)	^{13}C Enrichment (nM)		Pathways
			HL60	HL60-MX2	
Lactate	C2-C3	20.54	218	218.8	Glycolysis
Alanine	C2-C3	16.64	38	110.9	Glycolysis
Glutamate	C4-C5	33.93	78	194.9	Glycolysis & TCA
Glutamate	C2-C3	27.41	12	50.1	Glycolysis & TCA
Glycine	C2	41.91	8	45	Glycolysis & Glycine Synthesis
Aspartate	C2-C3	37		21.3	Glycolysis & Aspartate Synthesis
Serine	C2-C3	56.81	14.2	14.4	Glycolysis & Serine Synthesis
Serine	C2	56.81	2.2	18.5	Glycolysis & Serine Synthesis
Serine	C3	60.64	11.7	10.3	Glycolysis & Glycine Synthesis
Lactate	C1-C2-C3	68.95	21	17.2	Glycolysis & Aspartate Synthesis
Lactate	C2	68.95		1.5	Glycolysis & Serine Synthesis
Alanine	C3	16.64	3	6	Glycolysis & Serine Synthesis
Lactate	C3	20.54	4	2.7	recycle PPP & Serine Synthesis
Glutamate	C4	33.93	2	6.9	recycle PPP & TCA
Glutamate	C2	175.01	8	13.8	recycle PPP & TCA
Aspartate	C3	37		3.5	recycle PPP & Aspartate Synthesis
Aspartate	C2	52.65		10.8	recycle PPP & Aspartate Synthesis
Malate	C3	43.81	1.4	15.9	recycle PPP & enzyme malic
Glutamate	C3	27.41	13	68.5	2° turn TCA
Glutamate	C3-C4-C5	33.93		42.2	2° turn TCA
Glutamate	C1-C2	175.01	21	62.7	2° turn TCA
Glutamate	C1	175.01	4	12.3	2° turn TCA
Ribose-5-P	C1'(ATP)	87.28	60	73	PPP oxidative
Ribose-5-P	C1'-C2'(ATP)	87.28	58	98.7	PPP non oxidative
Ribose-5-P	C4'-C5' (ATP)	84.28	67	40.2	PPP non oxidative

Table 2. ^{13}C-labeled metabolites in HL60 and HL60-MX2 cell extracts.
In complex metabolic networks there will be a variety of isotopomers generated for each intermediate. Which isotopomers are present and their relative proportions are functions of the biochemical mechanism and metabolic fluxes. From these data it was possible to determine the isotopomeric distribution, isotopomeric ratio and metabolic networks that led to the production of these specific isotopomer pools.

Since cancer cells, as previously pointed out, show a common metabolic phenotype characterized by alteration of energy metabolism, we constructed a map of central metabolic network, including glycolysis, pentose phosphate pathway, TCA cycle and anaplerosis to characterize the phenotype of HL60 and HL60-MX2 cell line (Fig. 4). Thus, for the determination of metabolic profile of these lines, metabolites such ribose-5-P, lactate, glutamate, serine and glycine were taken into consideration. These metabolites can therefore be listed as biomarkers for the study of fluxes of substrates. (Tab. 3)

Each of the five conditions specified in table 3 rows are illustrated in figures 5, 6, and 7. In particular, the m_1 [1'-^{13}C]ribose-5-P ^{13}C was used to determine the relative contributions of oxidative PPP to ribose-5-P productions-P. The contribution of oxidative and non-oxidative PPP to R5P production can be estimated from m_2 and $m_{2'}$ribose-5-P isotopomers. If ribose-5-P is synthesized via the non-oxidative steps of PPP, the reactions catalyzed by the reversible transketolase and transaldolase lead to the production of m_2 [4',5'-^{13}C$_2$]- and $m_{2'}$[1',2'-^{13}C$_2$]ribose-5-P .

The contribution from the anaplerotic pathway versus the oxidative pathway, i.e. the pyruvate carboxylase (PC) activity (anaplerotic pathway) versus the pyruvate dehydrogenase (PDH) activity (oxidative pathway) can be expressed as a PC/PDH ratio, and calculated by $m_2/m_{2'}$ glutamate isotopomers ratio [16,4,26]. The flux ratio between glycolytic and pentose phosphate pathways can be expressed by the m_1[3-^{13}C]lactate isotopomer ratio. [17, 26, 29, 7, 6] The high flux of the pentose phosphate pathway accompanied by high serine synthesis from glycolysis intermediates, such as glycerate-3-phosphate, is compatible with a reduced glycolytic flux through the PGAM towards pyruvate and thus lactate synthesis. In leukaemia cells, when the flux through the pyruvate kinase is reduced, the production of the ATP required to satisfy energy demands in the synthesis of nucleic acids, proteins and lipids, should be dependent on the mitochondrial metabolism of the glutamine (glutaminolysis) [21]. This process strongly expressed in tumour cells. (see Figure 6)

Isotopomer ratio	Equation	HL60	HL60-MX2
Ribose from oxidative PPP (G6PDH activity) (Fig.6)	$$\dfrac{m_1\left[1'-^{13}C\right]Ribose-5-P}{\sum\limits_{i}^{n}m_i}$$	0.32	0.34
Ribose from non-oxidative PPP (TPI & TK activity) (Fig.6)	$$\dfrac{m_2\left[4',5'-^{13}C_2\right]Ribose-5-P}{\sum\limits_{i}^{n}m_i}$$	0.36	0.19
Ribose from non-oxidative PPP (TA & TK activity) (Fig.6)	$$\dfrac{m_{2'}\left[1',2'-^{13}C_2\right]Ribose-5-P}{\sum\limits_{i}^{n}m_i}$$	0.31	0.47
Contribution of anaplerosis to TCA cycle (PC & PDH activity) (Fig.5)	$$\dfrac{m_2\left[2,3-^{13}C_2\right]Glutamate}{m_{2'}\left[4,5-^{13}C_2\right]Glutamate}$$	0.15	0.26
Glycolityc and Pentose Phosphate Pathway activity (Fig.8)	$$\dfrac{m_1\left[3-^{13}C_2\right]Lactate}{\sum\limits_{i}^{n}m_i}$$	0.02	0.01

**Table 3. Isotopomer ratios in HL60 and HL60-MX2 cell lines.**

$\sum\limits_{i}^{n}m_i$ isotopomer is the sum of m_1, m_2, m_3,…m_n isotopomer of each metabolite analysed. The estimation of pentose cycle and glycolytic pathway activity was performed by isotopomer analysis of lactate and ribose-5-P. Briefly, when $[1,2-^{13}C_2]$glucose is used as the tracer, the activity of G6PDH will produce pentose phosphate labeled only in the C-1 position of pentose phosphate. This can be recycled to C-1, C-2, or C-3 of hexose phosphate and subsequently converted to $[3-^{13}C]$, $[2-^{13}C]$ or $[1-^{13}C]$lactate or alanine.
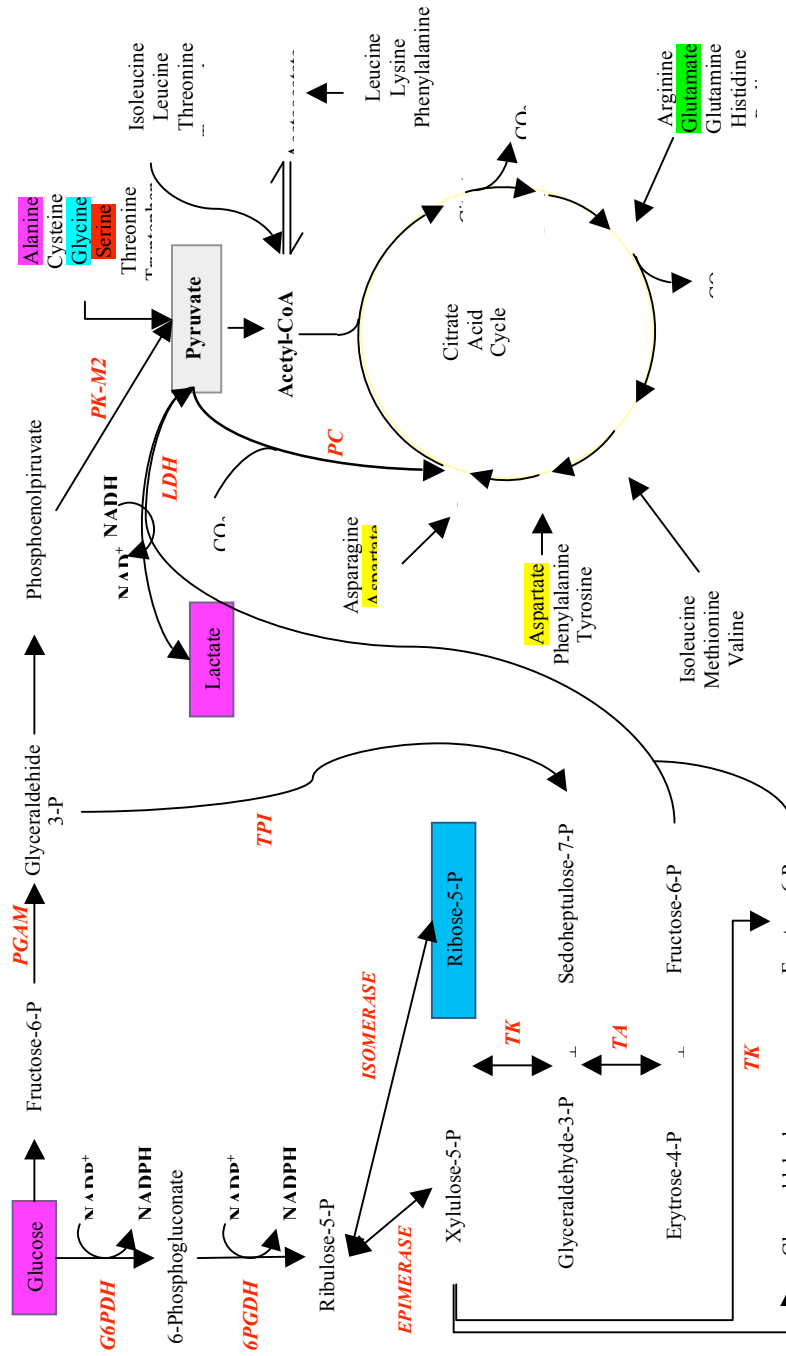
Figure 4. Main metabolic pathways for the cellular energy metabolism
. The dissection of central carbon metabolism into two subnetworks is apparent: glycolysis and pentose phosphate pathway take place in the cytosol, while TCA cycle takes place in the mitochondrial matrix. PGAM: phosphoglyceratemutase enzyme; M2-PK: pyruvate kinase enzyme isoform M2; LDH: lactate dehydrogenase enzyme PC: pyruvate carboxylase enzyme; PDH: pyruvate dehydrogenase enzyme; TPI: trioseophosphate isomerase enzyme; G6PDH: glucose-6-P dehydrogenase enzyme; 6PGDH: 6-phosphogluconate dehydrogenase enzyme; TK: transketolase enzyme; TA: transaldolasi enzyme.

3.2. Glucose utilization trough TCA cycle
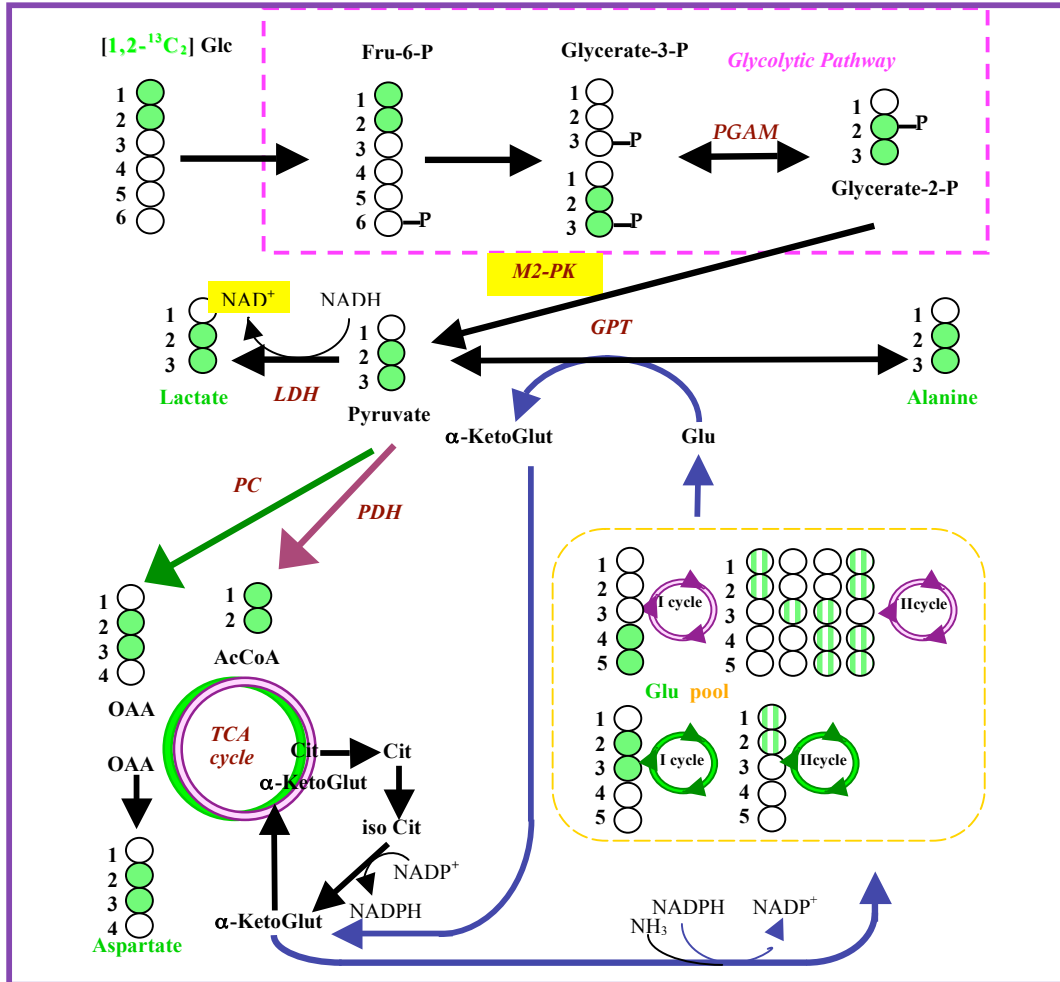
Figure 5. One possible Glycolitic pathway through which [1,2-^{13}C$_2$]glucose produces [2,3-^{13}C$_2$]pyruvate and, subsequently, lactate, alanine, oxaloacetate and acetyl-CoA.

This model agrees with a highly effective pyruvate kinase type M2 (M2-PK), which is generally over-expressed in all tumour cells and may be defined as a metabolic model that is dependent on NAD$^+$ production. The glutamate isotopomers labelling ratio (see Tab. 3), is indicative of a relatively higher PDH flux for pyruvate entry into the TCA cycle. The metabolic profile described herein may be representative of a subpopulation in stage G0/G1 of the cell cycle. It's important to note the presence of [2,3-^{13}C$_2$] aspartate isotopomer only in the ^{13}C spectra of HL60-MX2 cell extract . The aspartate is important for the nucleic acids synthesis, this synthesis is increased in resistant cell. (see Tab. 2)

3.3. Glucose utilization for nucleotides synthesis through the PPP (pentose phosphates pathway)
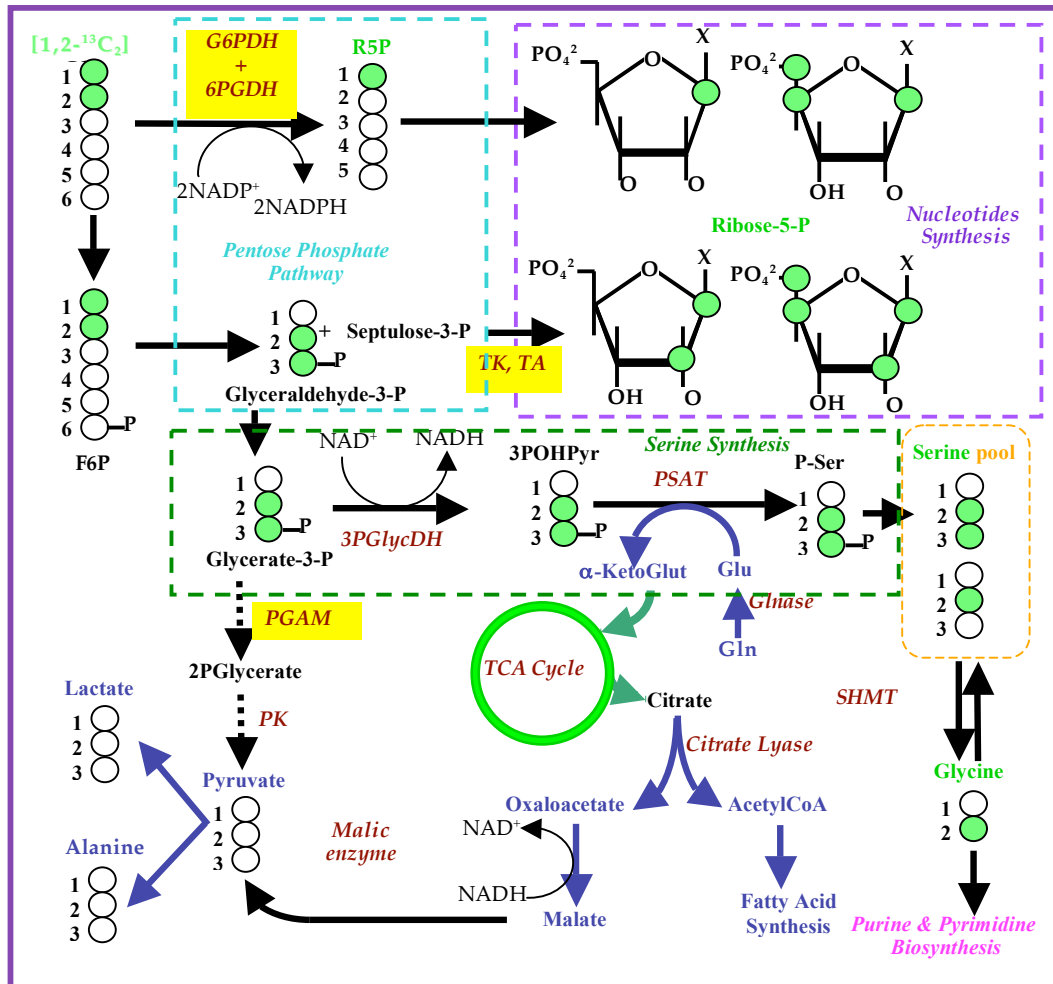
Figure 6. Production from 1,2-^{13}C$_2$]glucose of ribose-5-P isotopomers leading to free nucleotides (ATP, AMP, ADP, GTP, UDPG and IMP).

The production of isotopomers such as [1′-^{13}C]ribose-5-P and [1′,4′,5′-^{13}C$_3$]ribose-5-P is due to the direct oxidation of glucose in the pentose cycle through G6PDH activity. The production of [1′,2′-^{13}C$_2$]- or [1′,2′-4′,5′-^{13}C$_4$] Rib-5-P-nucleotides is evidence of ribose synthesis through TK of the non-oxidative pathway of the pentose phosphates pathway. The ribose isotopomers ratio are, respectively, indicative of oxidative and non-oxidative pentose phosphate pathway activity. In particularly in both cell lines there is a relatively higher non-oxidative synthesis of ribose-5-P (see Tab. 3). The metabolic profile described herein may be representative of a subpopulation mainly in stage G1/S of the cell cycle.

Pentose Recycling into pathway glycolytic and TCA cycle
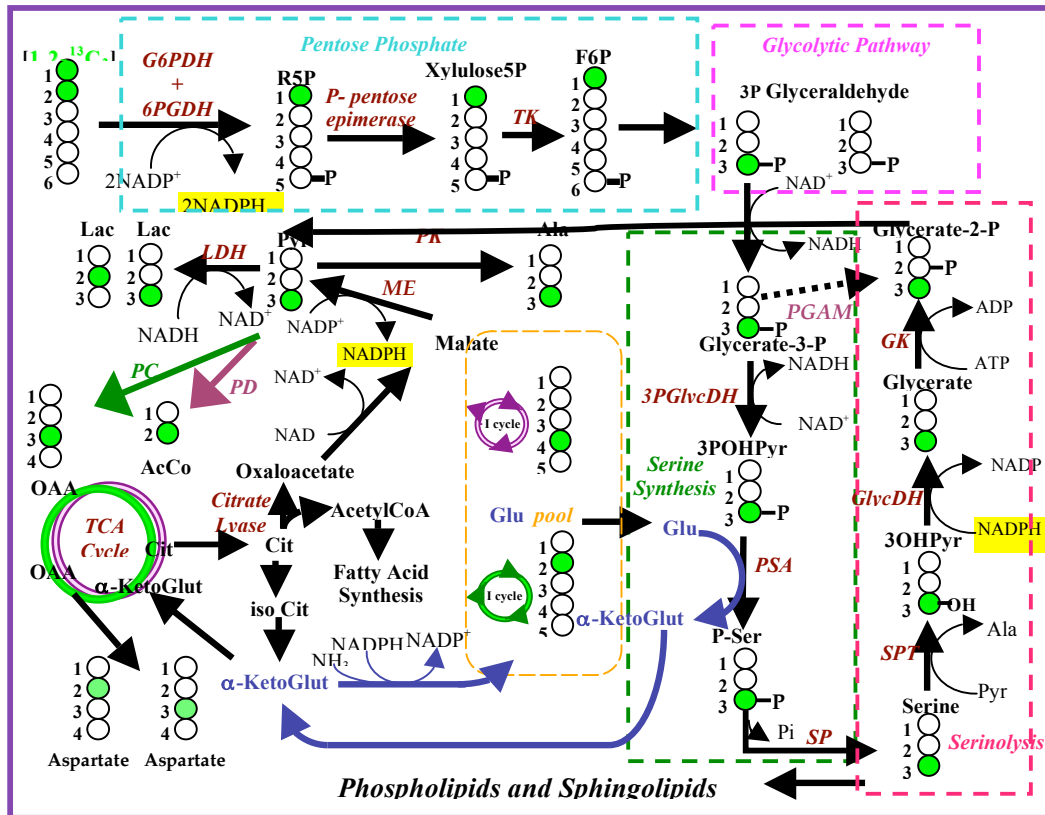
Figure 7. Production of ^{13}C labeled isotopomers in a single position.

This is in agreement with a metabolic framework characterized by a strong demand for NADPH production not associated with a comparable demand for phospho-ribose-pyrophosphate (PRPP) for nucleotide synthesis. This process may be ascribed to a cell subpopulation in the M phase of the cell cycle.
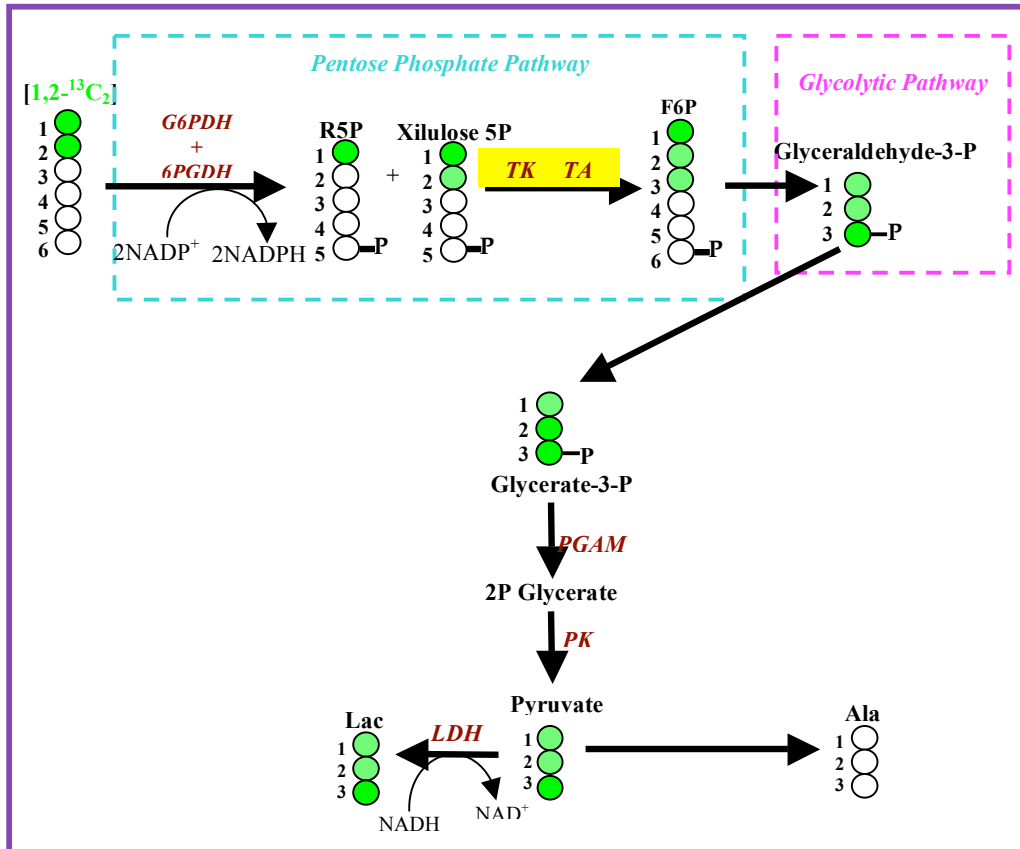
Figure 8. Production of isotopomer m_3 lactate in a subpopulation of cell in G0/G1 cell cycle phase.

This isotopomer reflects the activity of non-oxidative branch of the pentose phosphates pathway and the subsequent recycling of glycolytic intermediates $[1,2,3-^{13}C_3]$fructose, from pentose phosphates pathway into glycolysis. This glycolytic intermediate is formed from $[1,2-^{13}C_2]$fructose-6-P from glycolysis, which reacts with $[1-^{13}C]$ribose-5-P, to form $[1,2,3-^{13}C_3]$ sedeptulose-P-7 through TK and TA activities, and so $[1,2,3-^{13}C_3]$fructose-6-P and after $[1,2,3-^{13}C_3]$ lactate in the glycolysis. The m_1 lactate isotopomer ratio (see Table 3) confirms that in these two lines there is a greater TK and TA activities, recycling of pentose intermediates and increased non-oxidative synthesis of nucleotides. [12, 13]

4. DISCUSSION

The data reported in this work indicate:

i)   a high glycolytic and glutaminolytic activity;

ii)   an increased activity of enzymes TK + TA compared to that of the oxidative branch of pentose phosphates pathway;

iii)   an increased activity of PDH relative to PC in the use of glucose in the Krebs cycle.

Moreover, we reconstructed the metabolic pathways characterized by NAD^+ and $NADP^+$ dependence.[2]

The data show that in HL60-MX2 cell lines the non-oxidative synthesis of ribose-5-P prevails in the pentose phosphate pathway. The balance between oxidative and non oxidative branches of the pentose phosphate cycle is necessary to maintain the metabolic efficiency of the cancer cells for growth and proliferation, and the perturbation of this balance by using a multiple hit drug strategy, lead to metabolic inefficiency and cell death. The stronger the imbalance in pentose phosphate cycle in favour of the oxidative branch caused by the different drug combinations, the stronger the inhibition of cell proliferation. It has been shown in previous studies that metabolic adaptation of tumour metabolism includes an enhancement of pentose phosphate cycle fluxes and a specific balance between oxidative and non oxidative branches to maintain the high proliferative rates. The isotopomer ratio of ribose-5-P for the HL60-MX2 cell line indicates a higher flux in the pentose phosphate pathways than for the HL60 cell line.

The balance between oxidative and non oxidative branches of the pentose phosphate cycle is a vulnerable target within the cancer metabolic network for potential novel therapies in overcoming drug resistance. Thus, TK and TA enzymes could represent new targets for developing anticancer drugs. Our results are in agreement with the literature showing that changes in NAD^+ and $NADP^+$ levels can not only influence the cellular metabolism, in terms of growth and proliferation, but also activate or inhibit known anticancer agents such as doxorubicin.[4]

Glucose utilization, lactate production, and ATP content were higher in resistant cells due to a greater activity of mitochondrial hexokinase glyceraldehyde-3-phosphate dehydrogenase, malic enzyme, glucose-6-phosphate dehydrogenase, and 6-phosphogluconate dehydrogenase. In resistant cell, nucleic acids synthesis via the non-oxidative transketolase pathway is increased.[5,6,17] Cells which exhibited a (oxidative/non-oxidative) flux ratio for nucleic acid ribose synthesis of< 1 were resistant.

In summary, elevated glucose uptake and non-oxidative glycolytic metabolic phenotype can be used as sensitive markers for early detection of multidrug resistance in tumour cells.
The glutamate isotopomer ratio indicates a higher glutamate synthesis in HL60-MX2 cell than in HL60 ones. This increase in glutamate biosynthesis may serve as a detoxification mechanism to remove ammonia and to utilize enhanced production of NADPH, in resistant cells.

ACKNOWLEDGEMENTS

REFERENCE

1. Adiels M., Packard C., Caslake M.J., Stewart, P., Soro, A., Westerbakka J., Wennberg B., Olofsson S.-O., Taskinen, M.-R., and Boren, J. *A new combined multicompartmental model for apolipoprotein B-100 and triglyceride metabolism in VLDL subfractions. J Lipid Res* 46:58-67. (2005).

2. Ahmed N, Williams JF, Weidemann MJ. *Glycolytic, glutaminolytic and pentose-phosphate pathways in promyelocytic HL60 and DMSO-differentiated HL60 cells. Biochemistry and molecular biology International* 29, 6, (1993),1055-1067.

3. Aureli T., Di Cocco M.E., Calvani M., Conti F., *The entry of [1-^{13}C]glucose into biochemical pathways reveals a complex compartmentation and metabolite trafficking between glia and neurons: a study by ^{13}CNMR spectroscopy, Brain Res.* 765, (1997), 218–227.

4. Belfiore F., Borzi V., Lo Vecchio L., Napoli E., and Rabuazzo A. M. *Enzyme activities of NADPH-Forming Metabolic Pathways in Normal and Leukemic Leukocytes. Clin. Chem.* 21, 7, (1975) 880-883.

5. Boros L.G., Cascante M., and Lee P. W. N. *Metabolic Profiling of cell growth and death in cancer: applications in drug discovery.DDT* 7, 6, (2002).

6. Boros, L.G. *Metabolic targeted therapy of cancer: Current tracer technologies and future drug design strategies in the old metabolic network. Metabolomics* 1, (2005) 11-15.

7. Chen Yang, Richardson A. D., A. Osterman, J. W. Smith. *Profiling of central metabolism in human cancer cells by two-dimensional NMR, GC-_MS analysis, and isotopomer modeling. Metabolomics* 4, (2008) 13-29.

8. Dang, C.V. & Semenza, G.L. *Oncogenic alterations of metabolism. Trends Biochem. Sci.* 24, (1999) 68-72.

9. Eigenbrodt E, Kallinowski F, Ott M, Mazurek S, Vaupel P. *Pyruvate kinase and the interaction of amino acid and carbohydrate metabolism in solid tumors. Anticancer Res* 18 (1998), 3267–74.

10. Fan T. W.-M., Lane Andrew N.. *Structure-based profiling of metabolites and isotopomers by NMR. Progress in Nuclear Magnetic Resonance Spectroscopy* 52, (2008), 69-117.

11. Fiehn O et al.: *Combining genomics, metabolome analysis, and biochemical modelling to understand metabolic networks.* Comp. Funct. Genomics 2, (2001), 155-168.

12. Golub, T.R. et al. *Molecular classification of cancer: class discovery and class prediction by gene expression monitoring. Science* 286, (1999), 531-537.

13. Griffin J. L. & Shokcor J. P. *Metabolic profiles of cancer cells. Nat. Rev.* 4, (2004), 551-560.

14. Hellerstein, M. K. *New stable isotope-mass spectrometric techniques for measuring fluxes through intact metabolic pathways in mammalian systems: introduction of moving pictures into functional genomics and biochemical phenotyping.* Metab Eng 6, (2004), 85-100.

15. Irena Baranowska-Bosiacka[1]*, Bogusław Machaliński[2] and Jolanta Tarasiuk *The purine nucleotide content in human leukemia cell lines. Cellular & Molecular biology letters* 10, (2005),.217-226.

16. Kostrzewa-Nowak D., Paine M J I, Wolf and C R, Tarasiuk J**. The role of bioreductive activation of doxorubicin in cytotoxic activity against leukaemia HL60-sensitive cell line and its multidrug-resistant sublines. British Journal of Cancer 93,** (2005), 89-97.

17. Lee W.-N.P., Boros L.G., Puigjaner J., Bassilian S., Lim S., Cascante M., *Mass isotopomer study of the nonoxidative pathways of the pentose cycle with [1,2-13C2] glucose, Am. J. Physiol.* 274 (1998) 843–851.

18. Lee, W.N.P. *Characterizing phenotype with tracer based metabolomics. Metabolomics* 1, (2006), 31-39.

19. Malloy, C. R. Jones, J. G., Jeffrey, F. M., Jessen, M.E. and Sherry A., D. *Contribution of various substrates to total citric acid cycle flux and anaplerosis as determined by 13C isotopomer analysis and O2 consumption in the heart. Magma* 4, (1996), 35-46.

20. Malloy, C. R., Sherry, A. D., and Jeffrey, F. M. H. *Evaluation of carbon flux and substrate selection through alternate pathways involving the citric acid cycle of the heart by 13C NMR spectroscopy. J. Biol. Chem.* 263, (1988), 6964-6971.

21. Mazurek S, Eigenbrodt E. *The tumor metabolome. Anticancer Res.* 23, (2003),1149–54.

22. Mazurek S, Grimm H, Boschek CB, Vaupel P, Eigenbrodt E. *Pyruvate kinase type M2: a crossroad in the tumor metabolome. Brit J Nutr* 87, (2002), 23–9.

23. Mazurek S, Grimm H, Wilker S, Leib S, Eigenbrodt E. *Metabolic characteristics of different malignant cancer cell lines. Anticancer Res* 18, (1998), 3275–82.

24. Mazurek S, Michel A, Eigenbrodt E. *Effect of extracellular AMP on cell proliferation and metabolism of breast cancer cell lines with high and low glycolytic rates. J Biol Chem* 272, (1997), 4941–52.

25. Miccheli A., Puccetti C., Capuani G., Di Cocco M.E., Giardino L., Calzà L., Battaglia A., Battistin L., Conti F., *[1-¹³C] glucose entry in neuronal and astrocytic intermediary metabolism of aged rats. A study of the effects of nicergoline treatment by 13C NMR spectroscopy, Brain Res.* 966, (2003), 116–125.

26. Miccheli A., Tomassini A., Puccetti C., Valerio M., Peluso G., Tuccilli F., Calvani M., Manetti C., Conti F. *Metabolic profiling by ¹³C-NMR spectroscopy: [1,2-¹³C₂]glucose reveals a heterogeneous metabolism in human leukaemia T cells.* Biochimie 88, (2006), 437-448.

27. Schmidt K, Nørregaard LC, Pedersen B, Meissner A, Duus JO, Nielsen JO, Villadsen J. *Quantification of intracellular metabolic fluxes from fractional enrichment and 13C-13C coupling constraints on the isotopomer distribution in labeled biomass components.* Metab Eng. 1,2, (1999), 166-79.

28. Schuster, S., Dandekar, T. and Fell, D. A. *Detection of elementary flux modes in biochemical networks: a promising tool for pathway analysis and metabolic engineering.* Trends Biotechnol 17, (1999), 53-60.

29. Szyperski T. *Biosynthetically directed fractional ¹³C-labeling of proteinogenic amino acids. An efficient analytical tool to investigate intermediary metabolism. Eur. J. Biochem.* 232, (1995), 433-448.

30. Warburg O. *On the origin of cancer cells.* Science 123, (1956), 309–14.

31. Wiechert, W. and De Graaf, A. A. *Bidirectional reaction steps in metabolic networks I: Modeling and simulation of carbon isotope labeling experiments. Biotechnol Bioeng* 55, (1997), 101-117.

APPENDIX

1. Cell Culture

Human acute promyeloblast leukaemia cells, HL60 and HL60-MX2, were obtained from American Type Culture Collection (Manassas, VA) and were used within five passages. RPMI-1640 medium, glucose, sodium bicarbonate, sodium pyruvate, penicillin and streptomycin, L-glutamine, fetal bovine serum (FBS), trypan blue and NaOH were all from Sigma-Aldrich (ST. Louis, MI). 3-(trimethylsilyl)-tetradeutero-sodium propionate (TSP) was from Trimital (Milan, Italy).

Cellular models taken into account in this work are two promyeloblast human acute leukaemia cell lines, respectively, not resistant and resistant to several drugs (HL60 and HL60MX2). Cells were grown in $75cm^2$ tissue culture flasks with RPMI 1640 medium supplemented with 10mM glucose, 2mM glutamine, sodium pyruvate 1mM, sodium bicarbonate 2mg/ml, 100 units/ml penicillin, and 100μg/ml streptomycin and 10% FBS and were maintained in a humidified atmosphere of 95% air and 5% CO_2 incubator at 37°C. Cell growth and viability were evaluated by Trypan Blue exclusion test. Briefly, at the end of the experimental time 100μl of the cell suspension were mixed with 2% Trypan Blue and were counted in triplicate in a Burker camera under the optical microscope.

2. Analysis of cell cycle distribution by flow cytometry

For cell cycle analysis, cells were harvested, resuspended in cold PBS buffer and fixed with cold 70% ethanol for a minimum of 24 hours at 4 °C. Then $1-2 \times 10^6$ cells were washed twice in PBS and incubated with 2ml of 20μg/ml propidium iodide in PBS containing 0.002% Nonidet P 40 (Roche) and 12.5μg/ml RNase A (Sigma) at room temperature for a minimum of 60min. For each sample 20000 cells were analyzed for DNA content with a FACScan flow cytometer. The cell cycle analysis from the DNA histogram was determined by Modfit software (Becton Dickinson).(Fig.1a, b)
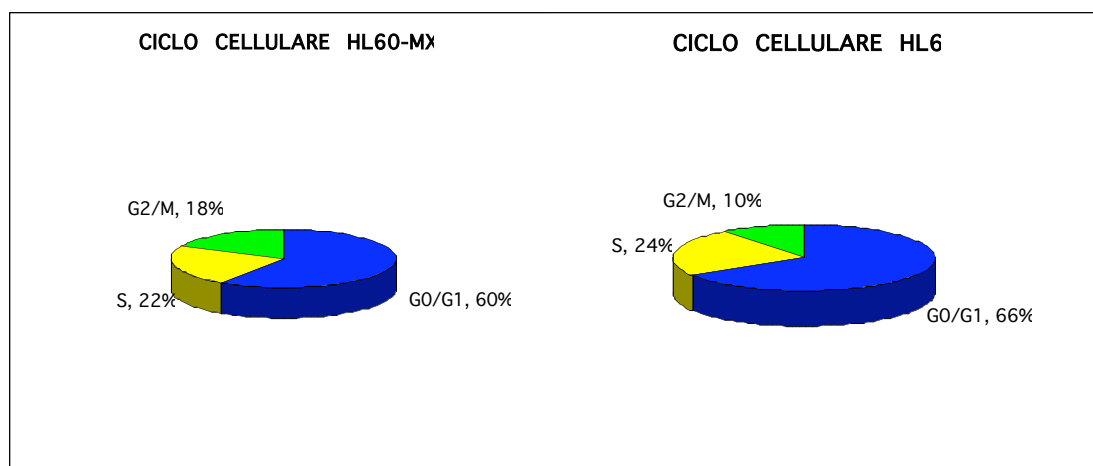
Figure A.1. a) Distribution of HL60 cell population into the cell cycle. b) Distribution of HL60-MX2 cell population into the cell cycle

3. *Experimental scheme, sample preparation for ^{13}C and NMR spectroscopy*

For ^{13}C-NMR experiments, 300×10^6 cells per sample were seeded at a starting density of 8×10^5 cells per ml and incubated for 24 hours in 60ml of complete medium added with ^{12}C-glucose 10mM (6 flasks representative of a control sample). In parallel 300×10^6 cells per sample were seeded at a starting density of 8×10^5 cells per ml and incubated for 24 hours in 60ml of complete medium added with $[1,2-^{13}C_2]$glucose (6 flasks representative of a ^{13}C labeled sample) in order to obtain an isotopic steady state labelling. The cells seed at 50% of confluence.

For ^{13}C-NMR spectroscopy, media and cell extracts were harvested after 24 hours culture. The cell pellets obtained were flash-frozen in liquid N_2 to minimize any metabolic change due to sample handling, freeze-dried, then polverized with pestle and extracted by Bligh-Dryer techniques as modified by us.(31,32). Briefly, were added to the cell pellets 2ml of cold CH_3OH, 2ml of cold $CHCl_3$ and 1ml of cold H_2O, incubate at 4°C for an hour and centrifuge at 10000 $\times$ g for 25 min. at 4 °C. The aqueous and lipid phases were taken up. The cell pellets were extracted again as previous described, incubated overnight at 4°C and centrifuged at 10000 $\times$ g for 25 min. at 4 °C again. The aqueous and lipid phases were taken up and combined with corresponding phases taken during the first

extraction, dried under N_2 flow and stored at $-80\ °C$ until NMR analysis. High-resolution ^{13}C-NMR spectra of cellular extracts were obtained on a Bruker Avance 500 spectrometer operating at $125.76\ MHz$ (^{13}C), respectively. Cell extracts were redissolved in $600\mu l$ of D_2O containing 0.15% ethylene glycol used as reference for chemical shift and concentration determination (^{13}C-NMR spectra).